ADCONIP 2014 Hiroshima

An Observer-based Input/output (I/O) Linearizing Control: Application to a EDC Vaporizer Unit

Kochnapoom Rungrueng and Chanin Panjapornpon

Abstract— **Coupled control of level and temperature of a vaporizer with heat integration is a challenging problem because the process is sensitive to disturbances resulting to a small stable operating regime. In this paper, an observer-based input/output (I/O) control system is proposed to handle both variables. The I/O linearizing controller provides a closed-loop desired tracking response with a few tuning parameters for stabilizing the process while the nonlinear observer with the linearizable error dynamics is applied to the control scheme for predicting compensated unmeasured states. The performance of the proposed control method is investigated through a case study of the 1,2-dichloroethane (EDC) vaporizer that has the liquid recirculation loop and the recovering heat from the furnace. The numerical simulation results show that the observer-based control system can handle the EDC vaporizer process efficiently for tracking setpoints and compensating unmeasured disturbances.**

I. Introduction

Petroleum and petrochemical industries have a complex process of which utility optimization, heat integration and recycle stream between units are essential keys to reduce operating costs. A vaporizer of a gas-liquid separation unit is an example that is usually associated with the process heat integration. A liquid stream fed to the vaporizer is boiled and evaporated by a preheater or heat recovery from other units. This unit needs to maintain the temperature and level of the vessel to generate a vapor flow and to pressurize downstream units which correspond to the operating conditions. Control of the vaporizer is a challenging task because the unit is in near unstable operating regime. If there is any disturbance occurred, e.g., temperature fluctuation in the furnace, it may cause instability of the unit and downstream.

From literatures, the control of the vaporizer process is not specifically mentioned but there are some works focused on the application of the gas-liquid separation process [1–5]. Grancharova et al. [1–2] studied the two-input and two-output (TITO) control problem of the laboratory-scale nitrogen oxide (NOx) reduction process with a liquid recirculating loop. The linear model predictive control (MPC) [1], and the linear MPC with orthogonal search tree partitioning [2] were applied for handling the pressure and level of the vessel by manipulating the vapor flow and liquid feed. Kocijan and Likar [3–4] developed the MPC with the Gaussian model to control the process in [1–2]. However, all of these mentioned works were focused on a two-state model that the dynamics of the gas density is neglected. Salcedo et al. [5] studied on the TITO control of a propane vaporizer using the generalized predictive controller with a linear parameter varying model (GPC-LPV); the three-state model of the level, temperature and gas density were considered. The liquid level and pressure in the vaporizer are the controlled outputs while the feed flow rate and heat power to the vaporizer are the manipulated variables. However, the robustness of the control method under process disturbance was not mentioned.

In this paper, the observer-based control system based on I/O linearization is proposed to handle two-input two-output vaporizer with both liquid recirculation loop and recovery heat from the furnace. The objective is to control the level and pressure of the vaporizer by adjusting the liquid feed and supplied energy. The proposed method can compensate state information to the I/O feedback when full measured states are not obtainable by integrating the nonlinear observer with linearizable error dynamics into the control system. An advantage of proposed observer-based controller is a few required tuning parameters to ensure the closed-loop stability of the near unstable system. Furthermore, there is no requirement of online optimization to obtain the control action.

This paper has the sections as follows. Scope and mathematical preliminaries are presented in section II. The observer-based control system design is shown in section III. Control performances of our proposed method compared with the I/O linearizing controller in Kanter's work [6] under an example of an EDC vaporizer are showed in section IV.

II. Scope and Mathematical Preliminaries

A. System Definition

Consider a class of nonlinear systems of the form:

$$\begin{aligned} \frac{dx}{dt} &= f(x,u) \\ y &= h(x) \end{aligned} \tag{1}$$

where $x=[x_1,...,x_n]^T \in X$ is the vector of state variables, $u=[u_1,...,u_m]^T \in U$ is the vector of manipulated inputs, $y=[y_1,...,y_m]^T$ is the vector of controlled outputs, and f and h are the smooth functions.

For the systems in (1), the relative orders of the controlled outputs, $y_1,...,y_m$, with respect to the inputs, $u_1,...,u_m$, are

Kochnapoom Rungrueng and Chanin Panjapornpon (corresponding author: 662-797-0999 ext. 1230; e-mail: fengcnp@ku.ac.th) are with Center of Excellence on Petrochemical and Materials Technology, Department of Chemical Engineering, Faculty of Engineering, Kasetsart University, Bangkok 10900, Thailand.

denoted by $r_1,...,r_m$, where r_i is the smallest integer such that $\partial[d^{r_i} y_i / dt^{r_i}] / \partial u \neq 0$. The following notation is used:

$$\begin{aligned} y_i &= h_i(x) \\ \frac{dy_i}{dt} &= \frac{\partial h_i}{\partial x}\frac{\partial x}{\partial t} = h_i^1(x) \\ &\vdots \\ \frac{d^{r_i-1} y_i}{dt^{r_i-1}} &= \frac{\partial h_i^{r_i-2}}{\partial x}\frac{\partial x}{\partial t} = h_i^{r_i-1}(x) \\ \frac{d^{r_i} y_i}{dt^{r_i}} &= \frac{\partial h_i^{r_i-1}}{\partial x}\frac{\partial x}{\partial t} = h_i^{r_i}(x,u) \end{aligned} \tag{2}$$

III. OBSERVER-BASED CONTROL SYSTEM DESIGN

The schematic diagram of proposed observer-based control system is shown in Fig. 1. The control system consists of the I/O feedback controller and nonlinear state observer with linearizable error dynamics. More details of the control system design are given as follows.

A. I/O feedback controller

For the system in the form of (1), the closed-loop responses of outputs are requested in linear form as follows:

$$\begin{aligned} (\varepsilon_1 \mathcal{D} + 1)^{r_1} y_1 &= y_{sp,1} \\ &\vdots \\ (\varepsilon_m \mathcal{D} + 1)^{r_m} y_m &= y_{sp,m} \end{aligned} \tag{3}$$

where $\mathcal{D} = \frac{d}{dt}$ is the differential operator, $y_{sp,1},\ldots,y_{sp,m}$ are the desired setpoints and $\varepsilon_1,\ldots,\varepsilon_m$ are tuning parameters that are used to adjust the speed of the output responses, $y_1,\ldots,y_m$, respectively. By substituting the definition in (2), one obtains:

$$\begin{aligned} h_1(x) + \binom{r_1}{1}\varepsilon_1 h_1^1(x) + \cdots + \binom{r_1}{r_1}\varepsilon_1^{r_1} h_1^{r_1}(x,u) &= y_{sp,1} \\ &\vdots \\ h_m(x) + \binom{r_m}{1}\varepsilon_m h_m^1(x) + \cdots + \binom{r_m}{r_m}\varepsilon_m^{r_m} h_m^{r_m}(x,u) &= y_{sp,m} \end{aligned} \tag{4}$$

where $\binom{a}{b} = \frac{a!}{(a-b)!b!}$

The static feedback controller (u) can be obtained by solving (4) and be expressed in following compact form:

$$u = \Psi(x, y_{sp}) \tag{5}$$

B. Nonlinear state observer with linearizable error dynamics

In this work, the nonlinear state observer is applied to estimate state information for the feedback controller in (5). Accuracy of the state prediction is generally depended on model quality and available output measurements. So, for the system with high process-model discrepancy due to uncertainties, we use the observer structure with linearizable error dynamics of (6) to estimate the compensated state variables from the measured outputs.

$$\begin{aligned} \dot{z} &= f(z + Ly, u) - Ly \\ \hat{x} &= z + Ly \\ \hat{y} &= h(\hat{x}) \end{aligned} \tag{6}$$

where the constant $[n \times m]$ matrices, L, are the observer gains, z is the vector of compensated state errors and $\hat{x}$ is the vector of estimated states.

C. Control system

To ensure offset-free response of the closed-loop system, a feedback compensator is added to eliminate the accumulation of error by adjusting the desired setpoint to the form

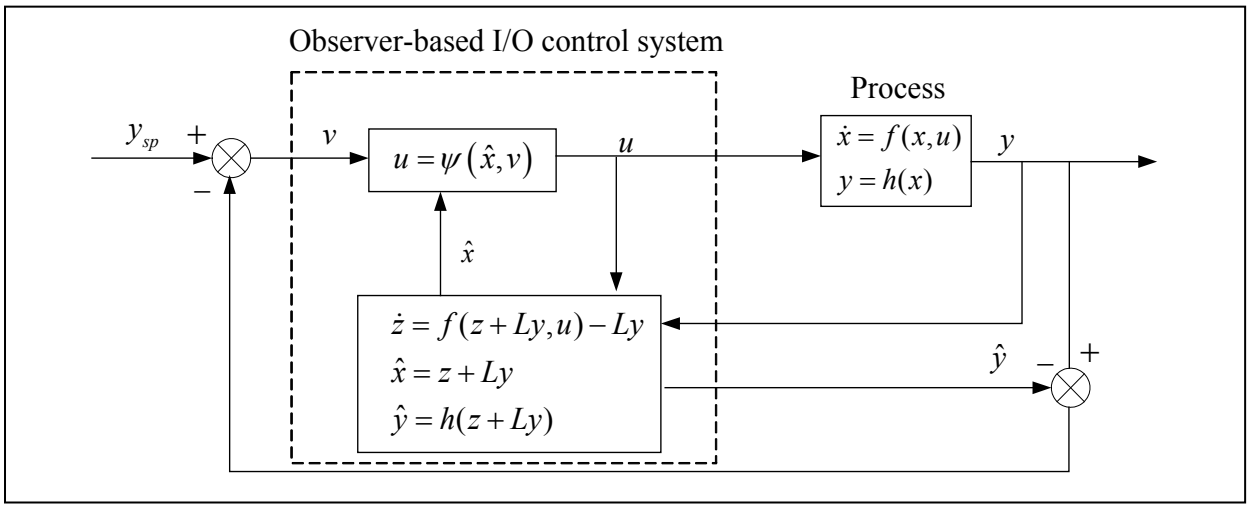

Figure 1. Schematic diagram of the proposed control system

$$v = y_{sp} - (y - \hat{y}) \tag{7}$$

where v is the vector of compensated setpoints.

By combining eqs. (5-7), the developed observer-based control system can be described by

$$\begin{aligned} \dot{z} &= f(z + Ly, u) - Ly \\ \hat{y} &= h(z + Ly, u) \\ u &= \Psi(z + Ly, y_{sp} - (y - \hat{y})) \end{aligned} \tag{8}$$

The observer gains (L) and feedback tuning parameters (ε) should be set such that the closed-loop process responses are asymptotically stable, which means all eigenvalues of the matrix in (9) are negative.

$$\left[\frac{\partial f}{\partial x} + \frac{\partial f}{\partial u}\frac{\partial \Psi}{\partial x} + \frac{\partial f}{\partial u}\frac{\partial \Psi}{\partial z} \right]_{x_{ss}, z_{ss}, u_{ss}} \tag{9}$$

IV. ILLUSTRATIVE EXAMPLE

In this paper, the EDC vaporizer with a liquid recirculating loop and heat recovery from the EDC cracking furnace is considered as a case study. The process scheme is shown in Fig. 2. The liquid EDC in the vaporizer is mixed with an EDC fresh feed and then flows through the top part of the furnace for recovering heat from the cracking furnace (Q_D). The hot fluid then passes through a heating zone to increase the fluid temperature before flashing in the vaporizer. The liquid EDC will be vaporized and vented out at the top. A mathematical model of the EDC vaporizer is derived from material and energy balances. Following assumptions are applied in modeling the system:

a) The average values of liquid density (ρ) and liquid heat capacity (c_p) within the operating temperature range are applied.

b) There is no reaction occurred in the system.

c) The cross-sectional area of the vaporizer (A) is constant.

d) Dynamics of the temperature in the gas phase is neglected. Thus, temperatures of both liquid and gas phase are in equilibrium.

By performing mass balance and energy balance in the liquid phase, dynamics of the vessel level and liquid temperature can be described as follows:

$$\frac{dh}{dt} = \frac{1}{\rho A}\left(F_i - W_v\right) \tag{10}$$

$$\frac{dT}{dt} = \frac{1}{\rho c_p A h}\left[c_p F_i \left(T_i - T\right) - W_v \lambda_v + Q + Q_D\right] \tag{11}$$

where h is the liquid level, ρ is the density of the liquid EDC, A is the cross-sectional area of the vaporizer, F_i is the EDC feed flow rate, W_v is the vaporization rate, T is the temperature in the vaporizer, c_p is the liquid heat capacity,

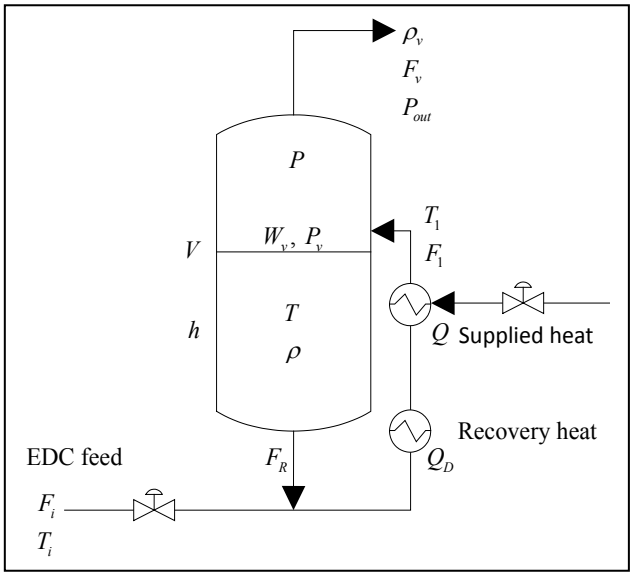

Figure 2. Schematic diagram of the EDC vaporizer

T_i is the EDC feed temperature, λ_v is the heat of vaporization of EDC, Q is the supplied heat and Q_D is the recovered heat.

For the mass balance in the gas phase, dynamics of the gas density is described as follows:

$$\frac{d\rho_v}{dt} = \frac{1}{\left(V - Ah\right)}\left[\rho_v\left(\frac{F_i}{\rho} - F_v\right) + W_v\left(1 - \frac{\rho_v}{\rho}\right)\right] \tag{12}$$

where V is the volume of the vaporizer, ρ_v is the density of the EDC gas and F_v is the volumetric flow rate of the outlet gas.

The vaporization rate (W_v) can be calculated by (13)

$$W_v = K_{MT}\sqrt{P_v - P} \tag{13}$$

where K_{MT} is the constant, P_v is the vapor pressure of EDC and P is gas phase pressure.

The Antoine equation used for calculating P_v is described as

$$P_v = e^{(A_1/T + A_2)} \tag{14}$$

where A_1 and A_2 are Antoine parameters of EDC.

Gas phase pressure is calculated by the ideal gas law

$$P = \frac{\rho_v RT}{M} \tag{15}$$

where R is the gas constant and M is the molecular weight of EDC.

The outlet gas volumetric flow rate (F_v) is calculated by (16)

$$F_v = \frac{1}{\rho_v}\left(K \cdot \sqrt{\Delta P}\right) \tag{16}$$

where K is vaporization constant, and ΔP is pressure drop across valve.

Thus, the state variables of the vaporizer consist of the liquid level ($x_1=h$), temperature ($x_2=T$) and gas density ($x_3=\rho_v$). The control objective is to handle the liquid level ($y_1=h$) and temperature ($y_2=T$) simultaneously by adjusting the EDC feed ($u_1=F_i$) and supplied heat ($u_2=Q$) at the steady state of y_{1sp}=4, y_{2sp}=480 (x_{1ss}=4, x_{2ss}=480, x_{3ss}=24.6, u_{1ss}=55.9, u_{2ss}=1.62x10^4). The process parameters are given in Table I. This given equilibrium is near unstable because the eigenvalues of the open-loop process are near zero (-0.10, 8e-7 and -0.003). The zero dynamics of this process (ζ) are described by

$$\frac{d\zeta}{dt} = \frac{1}{(V - Ay_{1sp})}\left[\zeta\left(\frac{K_{MT}\sqrt{e^{(A_1/y_{2sp}+A_2)} - \frac{\zeta R y_{2sp}}{M}}}{\rho}\right.\right. \\ \left.\left. - \frac{1}{\zeta}\left(K \cdot \sqrt{\Delta P}\right)\right) + K_{MT}\sqrt{e^{(A_1/y_{2sp}+A_2)} - \frac{\zeta R y_{2sp}}{M}}\left(1 - \frac{\zeta}{\rho}\right)\right] \tag{17}$$

The system is minimum-phase because an eigenvalue of zero at given setpoints is negative value (-0.09)

By applying the proposed control system in (8) with relative order of r_1=1 and r_2=1, the equations of the control system can be obtained:

$$\frac{dz_1}{dt} = \frac{1}{\rho A}\left[u_1 - \left(K_{MT}\sqrt{e^{(A_1/\hat{x}_2+A_2)} - \frac{\hat{x}_3 R \hat{x}_2}{M}}\right)\right](1 - L_1)$$

$$\frac{dz_2}{dt} = \frac{1}{\rho c_p A \hat{x}_1}\left[c_p u_1\left(T_i - \hat{x}_2\right) - \left(K_{MT}\sqrt{e^{(A_1/\hat{x}_2+A_2)} - \frac{\hat{x}_3 R \hat{x}_2}{M}}\right)\lambda_v \right. \\ \left. + u_2 + Q_D\right](1 - L_2)$$

$$\frac{dz_3}{dt} = \frac{1}{\left(V - A\hat{x}_1\right)}\left[\hat{x}_3\left(\frac{u_1}{\rho} - \frac{1}{\hat{x}_3}\left(K \cdot \sqrt{\Delta P}\right)\right)\right. \\ \left. + \left(K_{MT}\sqrt{e^{(A_1/\hat{x}_2+A_2)} - \frac{\hat{x}_3 R \hat{x}_2}{M}}\right)\left(1 - \frac{\hat{x}_3}{\rho}\right)\right] \\ - L_3\frac{1}{\rho A}\left[u_1 - \left(K_{MT}\sqrt{e^{(A_1/\hat{x}_2+A_2)} - \frac{\hat{x}_3 R \hat{x}_2}{M}}\right)\right] \\ - L_4\frac{1}{\rho c_p A \hat{x}_1}\left[c_p u_1\left(T_i - \hat{x}_2\right) - \left(K_{MT}\sqrt{e^{(A_1/\hat{x}_2+A_2)} - \frac{\hat{x}_3 R \hat{x}_2}{M}}\right)\lambda_v \right. \\ \left. + u_2 + Q_D\right]$$

$$\begin{aligned} \hat{y}_1 &= \hat{x}_1 \\ \hat{y}_2 &= \hat{x}_2 \\ \nu_1 &= y_{1sp} - \left(x_1 - \hat{x}_1\right) \\ \nu_2 &= y_{2sp} - \left(x_2 - \hat{x}_2\right) \\ u_1 &= \hat{W}_v + \rho A\frac{\left(\nu_1 - \hat{x}_1\right)}{\beta_1} \\ u_2 &= -Q_D - c_p u_1\left(T_i - \hat{x}_2\right) + \hat{W}_v \Delta H + \rho c_p A \hat{x}_1 \frac{\left(\nu_2 - \hat{x}_2\right)}{\beta_2} \end{aligned} \tag{18}$$

where

$$\begin{aligned} \hat{x}_1 &= z_1 + L_1 y_1 \\ \hat{x}_2 &= z_2 + L_2 y_2 \\ \hat{x}_3 &= z_3 + L_3 y_1 + L_4 y_2 \end{aligned}$$

V. CONTROL PERFORMANCE

To illustrate the control performances, the proposed control system and the mixed error and state-feedback I/O controller presented in the work of Kanter et al [6] are compared for both servo and regulatory tests. In servo test, the initial condition of the process is at $\left[h(0),\ T(0),\ \rho_v(0)\right] = [3.26,\ 450,\ 1.5]$. The set of tuning parameter values, ($\beta_1 = 100$ s, $\beta_2 = 100$ s, $L_1 = 0.3$, $L_2 = 0.1$, $L_3 = 0.1$ and $L_4 = 0.1$) for the proposed method and ($\beta_1 = 100$ s and $\beta_2 = 100$ s) for the Kanter's method, are applied in the test. The effects of tuning parameters to closed-loop eigenvalues are shown in Tables II-III. From Table II, it shows that an increase on β leads to the unstable of closed-loop eigenvalue. The smaller values of β are, the faster output responses to the desired setpoints become. The values of L that are stabilized the process are within a small range as shown in Table III. Increase on L will make the closed-loop eigenvalue becomes positive or complex, leading to an unstable system.

A. Servo performance

In the servo test, the setpoints are changed from y_{2sp}=480 K (u_{1ss}=55.9 kg/s and u_{2ss}=1.62x10^4 kW) to y_{2sp}=500 K (u_{1ss}=55.9 kg/s and u_{2ss}=1.82x10^4 kW) at t=1.1 hrs and from y_{1sp}=4 m to y_{1sp}=3 m at t=1.9 hrs. From Fig. 3, the results showed that both the proposed control system and the Kanter's controller successfully force the process outputs to track the setpoints with similar responses due to the use of the I/O feedback controller structure.

B. Regulatory performance

In the regulatory test, the setpoints are maintained at y_{1sp}=4 m and y_{2sp}=480 K. Then, the step disturbance of the heat recovery is added to the system at t=0.36 hrs to be Q_D=3000 kW. The proposed control system used the nonlinear observer with linearizable error dynamics which ensure the closed-loop stability of the near unstable system.

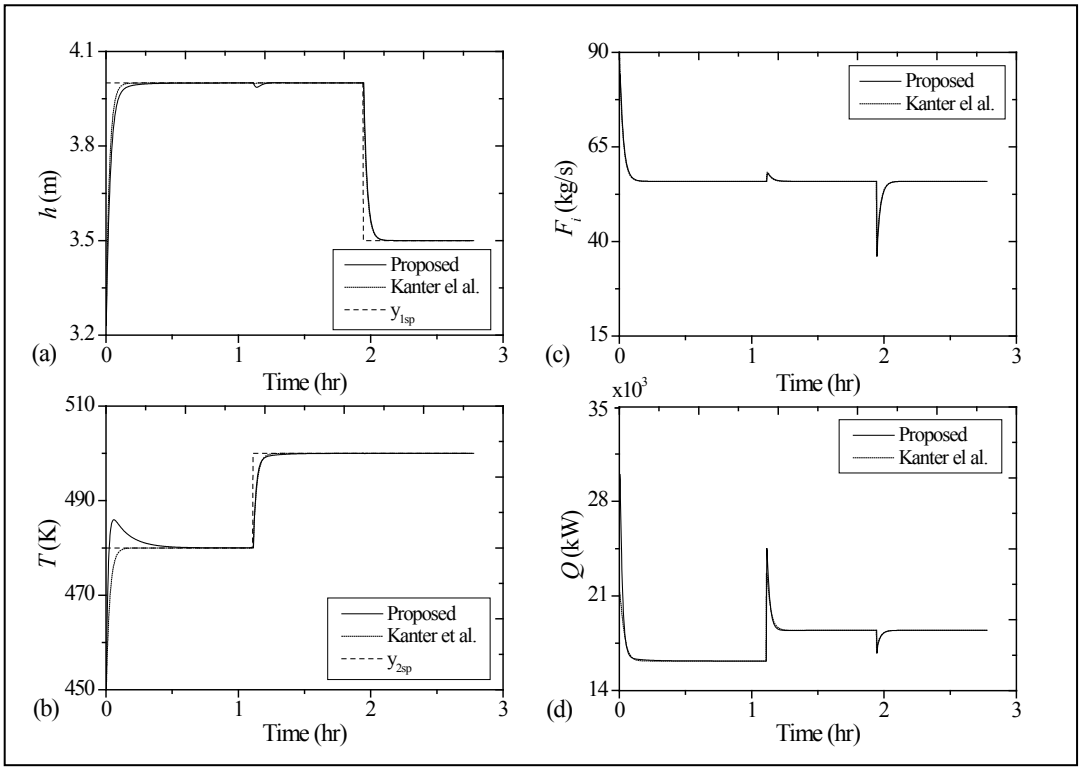

Figure 3. Servo performance of EDC vaporizer unit; (a) and (b) are response of output variables h and T, respectively. (c) and (d) are response input variables F_i and Q, respectively, in case of +20 step setpoint (y_2) at t=1.1 hr and -1 step setpoint (y_1) at t=1.9 hr.

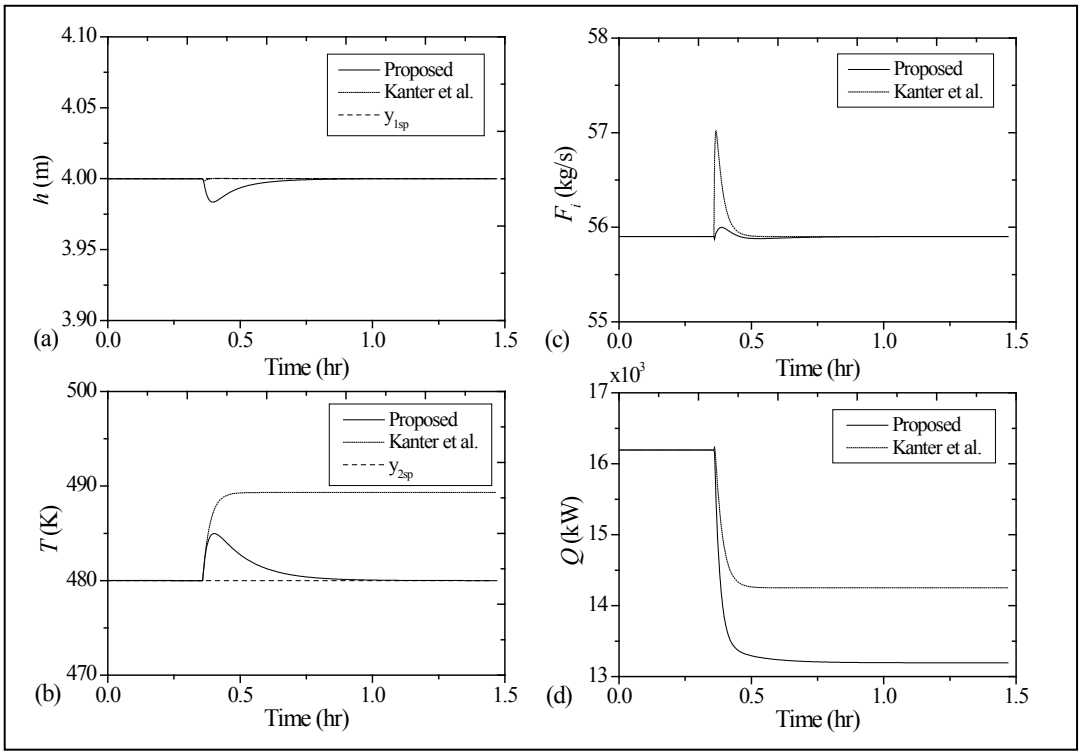

Figure 4. Regulatory performance of EDC vaporizer unit in case of heat disturbance Q_D=3000 kW is added to the system at t=0.36 hr; (a) and (b) are response of output variables h and T, respectively. (c) and (d) are response of input variables F_i and Q, respectively.

Table I. PARAMETER VALUES FOR THE EDC VAPORIZER

Parameter	Value	Units
A	4.31	m^2
A_1	-4149	
A_2	11.37	
c_p	2.0312	kJ/(kg.K)
K	25	$kg/(s \cdot \sqrt{bar})$
K_{MT}	24.16	$kg/(s \cdot \sqrt{bar})$
M	98.96	kg/kmol
R	8.314×10^{-5}	$m^3.bar/(mol.K)$
T_i	458	K
V	40	m^3
ΔP	5	bar
λ_v	245	kJ/kg
ρ	920	kg/m^3

Table II. THE EFFECT OF β TO CLOSED-LOOP EIGENVALUES

Tuning parameters	β_1	50	50	50	100	500
	β_2	50	100	500	100	100
	L_1	0.3	0.3	0.3	0.3	0.3
	L_2	0.1	0.1	0.1	0.1	0.1
	L_3	0.1	0.1	0.1	0.1	0.1
	L_4	0.002	0.002	0.002	0.002	0.002
Closed-loop eigenvalues	λ_1	-0.0813	-0.0811	-0.0200	-0.0820	-0.0828
	λ_2	-0.0747	-0.0747	-0.0001	-0.0759	-0.0769
	λ_3	-0.0003	-0.0002	-0.0020	-0.0002	-0.0100
	λ_4	-0.0063	-0.0066	-0.0069	-0.0049	-0.0001
	λ_5	-0.0200	-0.0100	-0.0747	-0.0100	-0.0035
	λ_6	-0.0200	-0.0200	-0.0809	-0.0100	-0.0020

Table III. THE EFFECT OF L TO CLOSED-LOOP EIGENVALUES

Tuning parameters	β_1	100	100	100	100	100
	β_2	100	100	100	100	100
	L_1	0.3	0.3	0.3	0.8	1.4
	L_2	0.1	0.2	0.4	0.1	0.1
	L_3	0.1	0.1	0.1	0.1	0.1
	L_4	0.002	0.002	0.002	0.002	0.002
Closed-loop eigenvalues	λ_1	-0.0820	-0.0822	-0.0804	-0.1024	-0.1870
	λ_2	-0.0759	-0.0461	-0.0194 + 0.0220i	-0.0847	-0.0850
	λ_3	-0.0002	-0.0160	-0.0194 - 0.0220i	-0.0158	-0.0213
	λ_4	-0.0049	0.0007	-0.0053 + 0.0036i	-0.0101	-0.0100
	λ_5	-0.0100	-0.0068 + 0.0013i	-0.0053 - 0.0036i	-0.0001	-0.0024
	λ_6	-0.0100	-0.0068 - 0.0013i	0.0023	-0.0032	0.0002

Thus, from Fig. 4, the results clearly showed that the proposed control system can significantly improve the control performance over Kanter's controller and can successfully eliminate the effect of the disturbance.

VI. CONCLUSION

The observer-based I/O feedback controller has been proposed to handle the process with the near unstable operating condition. The developed I/O linearizing controller guarantees closed-loop stability with a few tuning parameters while the nonlinear state observer with linearizable error dynamics provides compensated state information for the process. The control system has been tested with a case study of the EDC vaporizer of which the dynamics of the liquid level, vessel temperature and gas density are considered. The simulation results showed that the proposed control system provided a superior performance to handle the process efficiently despite the presence of unmeasured process disturbance.

ACKNOWLEDGMENT

This work was financially supported by the Graduate School, Kasetsart University, the project for Higher Education Research Promotion and National Research University Development, Office of the Higher Education Commission, and the Center of Excellence for Petrochemicals and Materials Technology. These supports are gratefully acknowledged.

REFERENCES

[1] Grancharova, A., Johansen, T.A., Kocijan, J., 2003. Explicit Model Predictive Control Of Gas-Liquid Separation Plant.

[2] Grancharova, A., Johansen, T.A., Kocijan, J., 2004. Explicit model predictive control of gas–liquid separation plant via orthogonal search tree partitioning. Computers & Chemical Engineering 28, 2481–2491.

[3] Kocijan, J., Likar, B., 2008. Gas–liquid separator modelling and simulation with Gaussian-process models. Simulation Modelling Practice and Theory 16, 910–922.

[4] Likar, B., Kocijan, J., 2007. Predictive control of a gas–liquid separation plant based on a Gaussian process model. Computers & Chemical Engineering 31, 142–152.

[5] Salcedo, J.V., Martínez, M., Ramos, C., Herrero, J.M., 2007. Predictive LPV control of a liquid–gas separation process. Advances in Engineering Software 38, 466–474.

[6] Kanter, J.M., Soroush, M., Seider, W.D., 2002. Nonlinear feedback control of multivariable non-minimum-phase processes. Journal of Process Control 12, 667–686.